

Enhanced Energy Management using Powertrain and Mission parameters : Case study of a Distributed Hybrid Propulsion Light Aircraft

Baptiste Legrand
 Université Franche-Comté,
 UTBM, CNRS, FEMTO-ST,
 Avions Mauboussin,
 Belfort, France,
 Email: baptiste.legrand@femto-st.fr

Arnaud Gaillard
 UTBM,
 CNRS, FEMTO-ST,
 Belfort, France

David Bouquain
 Université Franche-Comté,
 UTBM, CNRS, FEMTO-ST,
 Belfort, France

Abstract—Nowadays, the aeronautical field is transitioning from conventional fuel to electricity or hydrogen energy vectors. New environmental regulations constraining aircraft manufacturers push them towards new aircraft and powertrain architectures. These architectures largely differ from the current ones and require new design standards. All of the aircraft design stages are concerned. The research work presented in this article stems from a need of defining the influence of the Energy Management System on the early design stages. Previous work laid down the design basis. This paper showcases an energy management strategy associating powertrain and aircraft operation. Results over 5 flights highlight significant fuel savings as well as design discrepancies.

technology in the design of a distributed propulsion aircraft. The high volumetric power density of electric components enables a smooth integration of the drivetrains in or on the wing. Moreover these components high efficiency provides an interesting basis to improve aircraft operation flexibility at a low cost. The research presented hereafter is driven by such considerations. The energy management of a distributed hybrid electric propulsion aircraft is studied to highlight benefits of complex management strategies.

The energy management strategy presented here is referred as an AEMS. The AEMS aims to optimise the overall powertrain efficiency by trading with several parameters. These parameters can be related to the aircraft operation like speed or AoA, or the powertrain like battery SOC or drivetrain efficiency. This paper details the method, models and challenges associated with the development of an AEMS. Three AEMS using different management strategies are compared. This study aims to ascertain the feasibility, the performances and the limits of such AEMS. Section II provides a description of the aircraft and the powertrain. Section III introduces the simulation environment and the models. Section IV presents the AEMS design challenges and methods. Section V presents the results of the three AEMS studied.

NOMENCLATURE

η	Efficiency	<i>PES</i>	Primary Energy Supplier
<i>AC</i>	Aircraft	<i>rpm</i>	Rotation per minute
<i>AEMS</i>	Aircraft Energy Management Strategy	<i>SCS</i>	Source Control Strategy
<i>alt</i>	Altitude	<i>SOC</i>	State of Charge
<i>AoA</i>	Angle of Attack (°)	<i>T</i>	Traction
<i>BA</i>	Baseline	<i>TH</i>	Threshold
<i>CCS</i>	Consumer Control Strategy	<i>v</i>	Speed (m/s)
<i>DC</i>	Direct current	Subscripts	
<i>E</i>	Energy	<i>batt</i>	Battery
<i>FL</i>	Fuzzy logic	<i>C</i>	Correction
<i>FLP</i>	Flight plan	<i>dis</i>	Distributed
<i>m</i>	Mass flow (kg/h)	<i>drv</i>	Drivetrain
<i>N</i>	Rotational speed (rpm)	<i>kero</i>	Kerosene
<i>n</i>	Count of component	<i>mot</i>	Motor
<i>P</i>	Power (W)	<i>nom</i>	Nominal
		<i>prop</i>	Propeller

I. INTRODUCTION

Responding to new environmental constraints, the aeronautical research field is transitioning. New aircraft and powertrain architectures are actively researched. Examples of such concepts are distributed propulsion, hybrid powertrain, hydrogen engine, etc. [1], [2]. The goal is to develop a low carbon footprint aircraft achieving similar or better flight performance. Distributed propulsion is of interest as literature highlights significant benefits at the low speed [3] with similar performance at cruise speed. Hybrid electric powertrain is a key

II. AIRCRAFT AND POWERTRAIN CONCEPTS

A. Distributed propulsion aircraft

As introduced in section I, literature on distributed propulsion aircraft highlights several benefits regarding lift production [3] and empty weight [4]. In this study, the distributed propulsion is primarily used as a lift provider. The aircraft concept has been sized in a previous case study [5]. The aircraft has 10 to 12 seat, with a range of 1600km and a maximal speed of 306km/h. 32 propellers are distributed along the wingspan on the leading edge as highlighted in Fig.1. These propellers performance decrease at high speed, therefore a main propeller is added. The two resulting drivetrains are called distributed and main drivetrain.

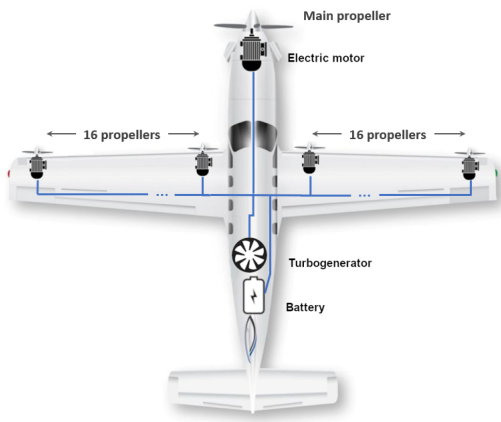


Fig. 1. Aircraft powertrain integration

Several powertrain architectures could be designed to propel the aircraft. Hybrid serie architectures are interesting due to their design and integration flexibility [6], [7]. Hybrid parallel architectures are interesting regarding their performance and mass savings [8]. In this paper, the powertrain studied is a hybrid serie. A battery pack is coupled to a PES composed of a turbine, two generators and their inverters. Two other architectures, hybrid serie with fuel cell and hybrid parallel with a turbine were sized but will not be discussed here.

B. Hybrid serie electric powertrain

As previously stated, the hybrid serie architecture has been selected for this paper. An electric schematic of the powertrain is proposed in Fig.2. The powertrain is composed of four systems : the battery, the PES, the distributed drivetrain and the main drivetrain. A reduction stage is integrated between the distributed propeller and motor. This component ensures that the motor speed does not exceed 6000rpm. A redundancy by design approach is taken regarding the powertrain. To do so, several components are parallelized such as turbine generator or main drivetrain inverters and motors. Consequently, only simultaneous component failures can lead to a complete loss of power during operation.

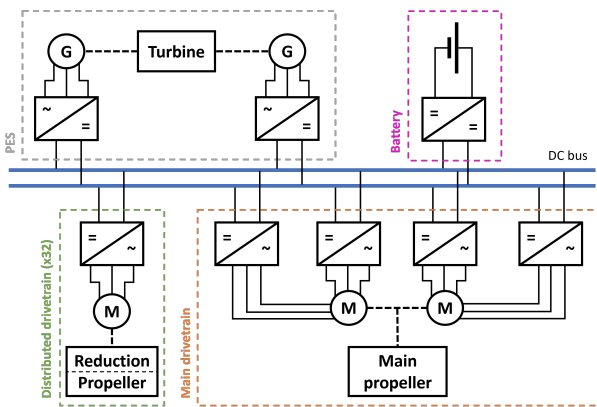


Fig. 2. Electric schematic of the hybrid serie powertrain

The characteristics of the selected components are shown in table I. The fuel tank can store up to 444kg of kerosene. The battery can store up to 44.3kWh of energy.

TABLE I
NOMINAL CHARACTERISTICS OF THE SELECTED COMPONENTS

System	Component	P_{nom}	N_{nom}	Selected component
PES	Turbine	296	2158	Arrius 1A
	Generator	200	2985	HPDM-250
	Inverter	112.5	-	CM200
Battery	Battery	354.1	-	VTC5A (185S-25P)
	Boost	500	-	DCUHV
Main drivetrain	Inverter	112.5	-	CM200
	Motor	230	4500	AXM4
Distributed drivetrain	Inverter	15	-	MC15
	Motor	6	6000	DHA

III. SIMULATION ENVIRONMENT

A. Aircraft models

The aircraft model computes the powertrain requirements based of the workflow detailed in Fig.3. First the lift and traction requirements are evaluated. The lift requirement is defined as the weight of the aircraft. This weight evolves during the mission as fuel is consumed. The traction requirement model accounts for the drag equilibrium, the ground friction, the aircraft acceleration and its breaking during landing.

The aeropropulsive model uses the lift and traction requirement to compute propeller traction requirements (T_{main} and T_{dis}) in two steps. Step one assesses the ratio of lift generated by the wing and by the distributed propellers. The lift generated by the wing is predicted using Prandtl lifting line theory. This theory [9] provides an accurate prediction of finite wing three-dimensions lift coefficient based on geometric characteristics such as wing span, chord width, wing profile lift coefficient, etc. Step two computes the traction the distributed and main drivetrains will generate to achieve the requirements. This calculation is based on the traction requirement and distributed propeller lift generation. The aeropropulsive model couples a model developed by Patterson et al. [10] and the Disk Actuator theory [11]. Patterson et al. model evaluates the propeller induced speed based on a lift requirement, speed, AoA and wing blown surface. The Disk Actuator theory predicts from the aircraft speed and propeller induced speed a traction requirement.

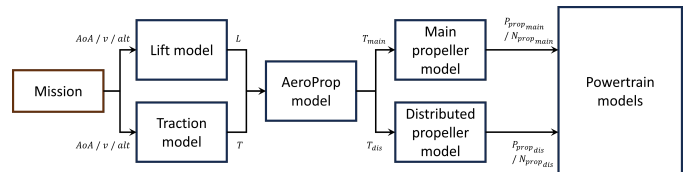


Fig. 3. Aircraft modelling workflow

As stated in section II, distributed propulsion is primarily used as a lift provider. The traction generated from the distributed propeller is seen as a byproduct. To achieve the traction requirement, the distributed propeller traction is balanced

with the main propeller traction. If the distributed propeller traction exceeds the traction requirements, an over traction phenomenon occurs.

Finally the propeller model uses a black box performance model from a manufacturer to define the propeller power, rotational speed and torque.

B. Powertrain model

The powertrain models are black box models provided by component manufacturers. The models gauge the components efficiency based on specific input data. The rotational speed and torque are used for electric machines. The power is used for the power electronics. The altitude and power are used for the turbine. Each component efficiency is used to predict the component input power. Higher fidelity models were also developed as a comparison basis. It stemmed from this comparison that higher fidelity models increased computation time while providing similar results as black box models. Therefore, black box models have been chosen to speed up the evaluation of AEMS design iterations.

IV. AIRCRAFT ENERGY MANAGEMENT SYSTEM

A. Case study objectives and challenges

Introduced in section I, the AEMS combines the energy management strategy and the aircraft operation. The development of autonomous vehicles in the automotive sector has shown interesting results [12]. Coupling trajectory optimisation and energy management is still unconventional in aeronautics despite extensive research on both topics. Therefore, this study has two main objectives. The first objective is to assess the performance three AEMS designed. The second objective is to prove the feasibility of the aircraft operation and energy management combination. The benefits and current limitations of these strategies will also be presented.

B. AEMS structure

The AEMS is structured as a multi-layered management system. The three AEMS compared are refereed as baseline (BA-AEMS), threshold (TH-AEMS) and fuzzy logic (FL-AEMS). Table II summarizes the first AEMS layer and primary functions shared by the three AEMS. Three states were identified : idle ground, ground roll and in flight.

TABLE II
FUNCTIONS INTEGRATED IN THE AEMS STATE-MACHINE

Function	Idle ground	Ground	In flight
Powering turbine	On/Off	Off	Off
Distributed propulsion	Off	On/Off	On
AoA lift correction	Off	Off	On
Aircraft breaking	On/Off	On	On

Turbine powering starts and stops the turbine during the idle ground phase. Distributed propulsion powers on or off the whole distributed drivetrain. This function is implemented to avoid over traction in specific cases. AoA lift correction corrects the AoA when the aircraft generates too much lift. Aircraft breaking activates the breaks during the landing.

Fig.4 provides an insight on the AEMS integration in the simulation environment. The first layer AEMS functions are highlighted in blue. Differences arise in the second management layer where the CCS and SCS modules are implemented. Their strategies are detailed in section IV-D and IV-E. The BA-AEMS is used as a control sample. Therefore for BA-AEMS, the CCS and SCS modules are disabled so AoA_{Cltf} , P_{CPES} and $n_{Cdrvdis}$ are 0. A low pass filter is added to represent the turbine response time.

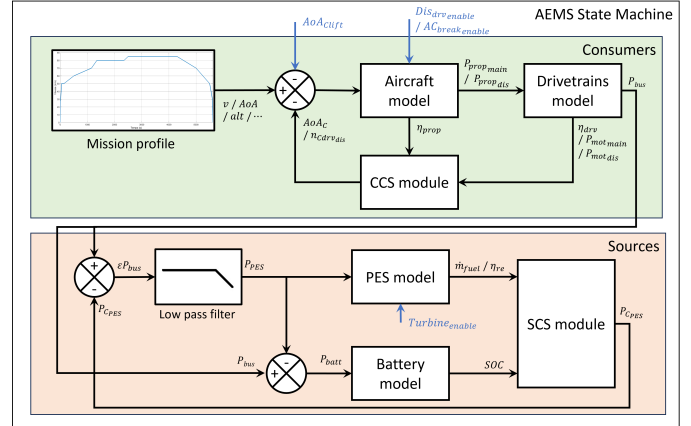


Fig. 4. Representation of the AEMS

C. Threshold and fuzzy logic : benefits and limits

Energy management strategies are usually split in two categories [13]. The optimization-based strategies strive to reach an optimal operating point with specific mission conditions. The rule-based strategies use a set of rules to manage the system. Despite being less than optimal by nature, rule-based strategies often provide similar or better results than optimization-based strategies when the latest are tested outside their optimized missions. Moreover, rule-based management are easier to predict which greatly simplifies certification procedures.

In this work, the threshold algorithms have been selected for their simplicity of integration and use. Three limits were identified for these algorithms. Firstly the instabilities might appear. Secondly when managing the system requires monitoring multiple variable, complexity of the algorithm rapidly increase. Thirdly, simple threshold value algorithm only return one correction value, limiting the system management. Fuzzy logic was selected as it is not subjected these three limits [14], [15]. However, this strategy requires a higher computing time and it is less predictable than the threshold algorithms.

D. Consumer Control System (CCS)

The CCS manages the main and distributed drivetrains. Reducing the energy consumption of these systems requires improving their combined efficiency. In this work, two strategies have been identified :

- 1) Change the power split between the main and distributed drivetrains (used in TH-AEMS and FL-AEMS)

- 2) Change the power split between the 32 distributed drivetrains (used in FL-AEMS)

Option 1) works on the basis that the aircraft has two lift providers. The wing is the first lift provider and the distributed propulsion is the second lift provider. Wing lift is conditioned by several parameters including the AoA. The control scheme can be summed as the following sequence :

- 1) Reduction of the AoA
- 2) Lower wing lift
- 3) Modification of lift balance
- 4) Higher distributed propeller induced speed and traction
- 5) Modification of drivetrains traction balance
- 6) Different drivetrains power split

Option 2) can be achieved by a modification in the number of active distributed drivetrains. This change leads to a different wing blown surface. An unwanted consequence of this is a modification in the propeller traction requirement. Lowering the wing blown surface induces a non proportional increase of propeller rotational speed and torque.

A hysteresis controller is used to model the TH-AEMS CCS. The correction is conditioned by the main drivetrain efficiency. As soon as the main drivetrain efficiency falls below 75%, a 2° AoA correction is applied. When the main drivetrain efficiency rises above 78% the controller disables the correction. The TH-AEMS CCS is disabled during the approach flight phase to avoid over correcting the system.

In the case of FL-AEMS, several combinations of option 1, 2 and a fuzzy logic controller were tested. However, such approach appeared detrimental to the energy consumption. Therefore, it has been decided that the two problems will be taken independently. Two variable gains were implemented. They are based on the correction curves in Fig.5. The two input data monitored are the distributed motor normalized power and the main motor normalized power.

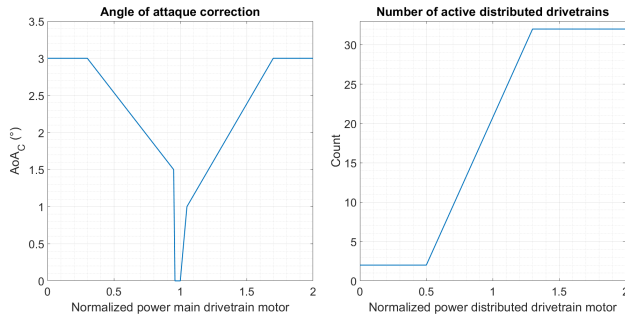


Fig. 5. CCS optimal control curves

E. Sources Control System (SCS)

The SCS manages the battery and the PES. The energy consumption reduction is also driven by the improvement of the combined systems efficiency. The two following strategies have been identified :

- 1) PES maximal efficiency (used in TH-AEMS)
- 2) Battery maximal depletion (used in FL-AEMS)

Option 1) strives to improve the PES efficiency on the whole mission profile. Therefore, when the power requirement exceeds the best PES efficiency power, fuel flow is lowered and the battery compensate the power requirement over time.

Option 2) strives to deplete the battery as much as possible. In this case, the battery provides energy even though the PES operates below its best efficiency power. The performance of the battery system is taken advantage of to increase the combined source efficiency.

A hysteresis controller is used to represent the TH-AEMS SCS. The correction is conditioned by the SOC which must remain above 0.3. The hysteresis controller applies a correction of 50kW when PES efficiency fall below 24% efficiency. When the PES efficiency rises above 25% the controller disables the correction.

Fig. 6 showcases the fuzzy logic input data membership functions. The two input data monitored are the SOC and the normalized turbine fuel flow.

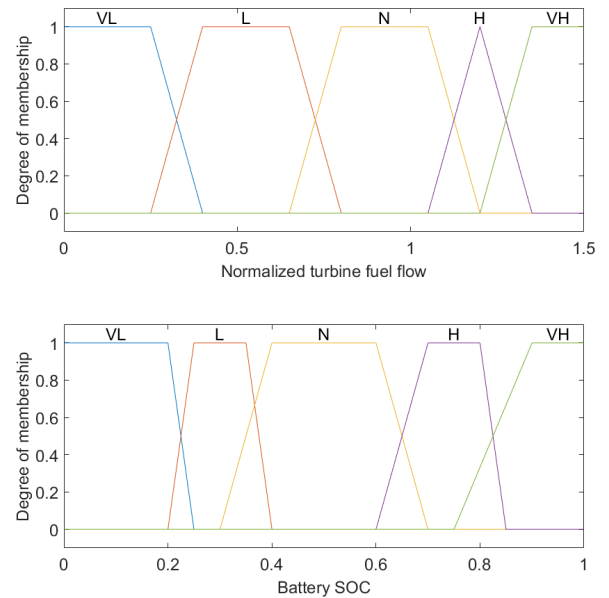


Fig. 6. SCS fuzzy logic input

Fig. 7 showcases the fuzzy logic output membership functions. $P_{C_{PES}}$ can be corrected up to 100kW. A recharge can also be proposed as the VL and L membership functions return a negative correction.

V. CASE STUDY RESULTS

A. Mission profile and objectives

The mission profile presented hereafter is FLP1. This profile mixes tourism and business applications with different flight conditions. The mission profile is composed of 5 flights. Table III shows the constraints applied to the flights.

Two other mission profiles FLP2 and FLP3 were tested but will not be detailed here. Therefore a total of 21 flights were

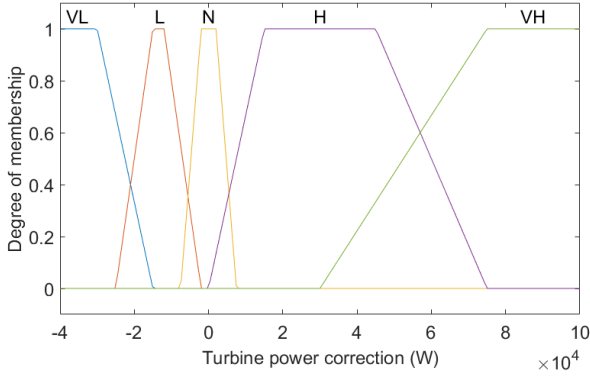


Fig. 7. SCS fuzzy logic output

TABLE III
FLP1 FLIGHT CONSTRAINTS

	Minimal	Maximal	Unit
Range	280	815	km
Altitude	3500	10000	ft
Cruise speed	252	288	km/h
Take-off / landing speed	126	137	km/h
Climb rate	437	560	ft/min
Descent rate	375	453	ft/min

tested. The aircraft fuel tank and battery are considered full at each take-off.

Several objectives can be factored in the study of energy management such as energy consumption, component ageing, powertrain cost, etc. For this study, the main driver is the energy consumption.

B. AEMS and mission influence

Overall, two different major results were investigated during the study. The first result is the influence of the flight duration on the fuel savings. Higher fuel savings are usually achieved with shorter flights. Using the FL-AEMS algorithm, fuel savings of 4.3% and 8.4% were achieved for the first and fourth flight. The first flight is 815km while the fourth flight is 407km long. The second result transcribes the effectiveness of the energy management. The metric used is the fuel energy saved per kWh of battery energy used. The higher the number, the more relevant the battery use is. For FLP1, TH-AEMS returns 6.8, while the FL-AEMS returns 3.5. From these results, it appears that this metric is mostly influenced by the energy management scheme. Table IV showcases the overall the fuel savings for FLP1. The battery maximal depletion strategy highlights better fuel savings than the maximal PES efficiency.

TABLE IV
COMPARISON OF ENERGY SAVINGS BETWEEN BA, TH AND FL AEMS

AEMS	$E_{Kero}(kWh)$	$E_{Batt}(kWh)$	Fuel saved
BA	9160	0.3	0%
TH	8907	37	2.8%
FL	8635	151	5.7%

Fig. 8 showcases the inputs and outputs of the CCS algorithm. From these figures, it appears that the TH-AEMS CCS corrects the AoA over longer periods of time. This increases the use of the distributed propulsion over the whole mission profile. The FL-AEMS showcases more variability in the AoA correction. Moreover, the variability of the number of distributed propellers used induces a motor power ratio closer to 1. From these results, the distributed propulsion design point can be questioned. A relaxed take-off constraint to lower the number of propellers could lead to a lighter and more efficient aircraft.

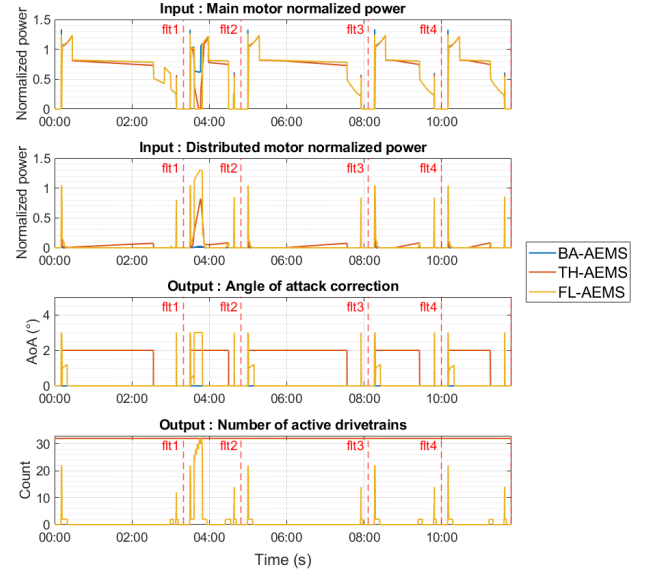


Fig. 8. CCS module input and output values

Fig. 9 showcases the inputs and output of the SCS algorithm. Three observations are made. First, instabilities are observable with the TH-AEMS correction. On the other hand, the FL-AEMS remains stable. Secondly, the three strategies accurately limit the battery SOC above 0.3. The BA-AEMS and TH-AEMS battery retains a lot of energy as their minimal SOC are around 0.98 and 0.8. A different battery design could benefit such strategy by reducing the battery mass. However, the battery C-rate must remain within acceptable margins. This might limit the battery mass reduction. The FL-AEMS reaches the 0.3 battery SOC where it is considered depleted. This depletion enables the energy savings previously illustrated. Thirdly, during the descent and approach, the FL-AEMS slightly recharges the battery. This function has been added to increase the battery SOC when the turbine operates at low efficiency due to a low fuel flow supply.

C. CCS limitations and further work

Section V-B highlights significant fuel savings using the TH-AEMS and FL-AEMS. This section also highlights that the CCS choice can lead to different uses of the distributed drivetrains. Moreover, the effectiveness of the CCS can be

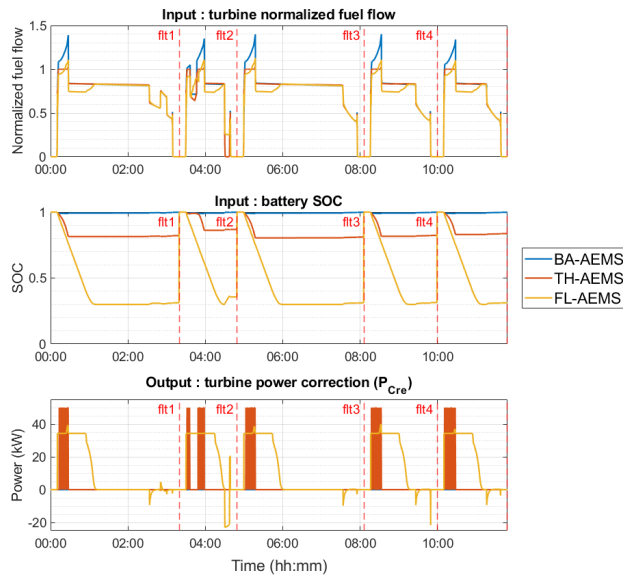


Fig. 9. CCS module input : turbine normalized fuel flow

questioned. A first quantification of the current CCS highlights that the strategy accounts for 14% to 14.5% of the fuel savings previously shown. The main factor in this result is the propeller performance. Distributed propeller is designed to be more efficient than main propeller under 235km/h. This condition is achieved for 12% to 28% of the flights in FLP1. Outside of this range, the CCS becomes either ineffective or even detrimental to the energy consumption reduction objective.

Based on this first proof of concept, two research questions are considered. The first question is to quantify the influence of other aircraft parameters like speed on the CCS correction. Fuzzy logic will be used to propose an AoA correction based on these multiple factors. The second research question aims to analyse the sensitivity of the CCS regarding other components or even other architectures. Fully distributed propulsion configuration might be designed at this hand.

VI. CONCLUSION

This paper presents a comparison of three AEMS for a distributed hybrid propulsion aircraft. The aircraft and powertrain concepts and models are introduced. Following this introduction, the AEMS design strategy is detailed. The specifics of the CCS and SCS modules are then detailed. These two management strategies, optimize the power split and energy flow of respectively the consumers (drivetrains) and the sources. The specificity of this work revolves around the use of aircraft parameters to operate one of the control strategies.

One mission profile containing 5 flights is tested. The optimized AEMS (TH and FL) respectively showcased fuel savings of 2.8% and 5.7%. It has also been highlighted that shorter flights and higher battery depletion will lead to higher fuel savings. Moreover, the different AEMS strategies

highlight the limits of the preliminary design. The battery sizing and number of distributed motors could be modified to reduce weight and improve the aircraft performance.

This study also highlights limits in the optimal management strategies like the CCS design. As stated, following work will focus on improving the CCS from other angles. Firstly, other parameters like aircraft speed will be accounted for in the CCS. Secondly, other components or aircraft configurations will be tested.

ACKNOWLEDGMENT

This work has been supported by the EIPHI Graduate School (contract ANR-17-EURE-0002), the Region Bourgogne Franche-Comté and Avions Mauboussin.

REFERENCES

- [1] P. D. Bravo-Mosquera, F. M. Catalano, and D. W. Zingg, "Unconventional aircraft for civil aviation: A review of concepts and design methodologies," *Progress in Aerospace Sciences*, vol. 131, p. 100813, 2022. [Online]. Available: <https://www.sciencedirect.com/science/article/pii/S0376042122000070>
- [2] B. J. Brelje and J. R. R. A. Martins, "Electric, Hybrid, and Turboelectric Fixed-Wing Aircraft: A Review of Concepts, Models, and Design Approaches," *Progress in Aerospace Sciences*, vol. 104, pp. 1–19, Jan. 2019.
- [3] R. de Vries and V. R., "Aerodynamic performance benefits of over-the-wing distributed propulsion for hybrid-electric transport aircraft," *Journal of Aircraft*, 2023.
- [4] H.-J. Steiner, C. P. Vratny, C. Gologan, K. Wieczorek, T. A. Isikveren, and M. Hornung, "Performance and Sizing of Transport Aircraft Employing Electrically-Powered Distributed Propulsion," in *61. Deutscher Luft- und Raumfahrtkongress 2012*, 2012.
- [5] B. Legrand, N. Curlier, A. Gaillard, and D. Bouquain, "High-level sizing method for hybrid electric distributed propulsion aircraft," in *Aerospace Europe Conference 2023*, 2023.
- [6] C. C. Chan, "The state of the art of electric, hybrid, and fuel cell vehicles," *Proceedings of the IEEE*, vol. 95, no. 4, pp. 704–718, 2007.
- [7] P. Saenger, K. Deschinkel, N. Devillers, and M.-C. Pera, "An optimal sizing of electrical energy storage system for an accurate energy management in an aircraft," in *2015 IEEE Vehicle Power and Propulsion Conference (VPPC)*, 2015, pp. 1–6.
- [8] F. D. Finger, C. Braun, and C. Bil, "An initial sizing methodology for hybrid-electric light aircraft," in *2018 Aviation Technology, Integration, and Operations Conference*, 2018.
- [9] J. D. Anderson, *Aircraft Performance and Design*. McGraw Hill, 1999.
- [10] M. Patterson, J. Derlaga, and N. Borer, "High-lift propeller system configuration selection for nasa's sceptor distributed electric propulsion flight demonstrator," in *16th AIAA Aviation Technology, Integration, and Operations Conference*, Jun 2016. [Online]. Available: <https://doi.org/10.2514/6.2016-3922>
- [11] P. R. Spalart, "On the simple actuator disk," *Journal of Fluid Mechanics*, vol. 494, p. 399–405, 2003.
- [12] J. Li, X. Wu, and J. Fan, "Speed planning for connected and automated vehicles in urban scenarios using deep reinforcement learning," in *2022 IEEE Vehicle Power and Propulsion Conference (VPPC)*, 2022, pp. 1–6.
- [13] P. Zhang, F. Yan, and C. Du, "A comprehensive analysis of energy management strategies for hybrid electric vehicles based on bibliometrics," *Renewable and Sustainable Energy Reviews*, vol. 48, pp. 88–104, 2015. [Online]. Available: <https://www.sciencedirect.com/science/article/pii/S1364032115002464>
- [14] S. N. Motapon, L.-A. Dessaint, and K. Al-Haddad, "A comparative study of energy management schemes for a fuel-cell hybrid emergency power system of more-electric aircraft," *IEEE Transactions on Industrial Electronics*, vol. 61, no. 3, pp. 1320–1334, 2014.
- [15] N. Noura, L. Boulon, and S. Jemei, "Real time performance estimation for energy management of a fuel cell hybrid electric vehicle," in *2021 IEEE Vehicle Power and Propulsion Conference (VPPC)*, 2021, pp. 1–5.